THE JOURNAL OF PHYSICAL CHEMISTRY Letters

Letter

Cite This: J. Phys. Chem. Lett. 2018, 9, 1229−1236

pubs.acs.org/JPCL

# Combined Experimental−Theoretical Study of the OH + CO → H + $CO_2$ Reaction Dynamics

Adriana Caracciolo,[†,#] Dandan Lu,[‡,#] Nadia Balucani,[†] Gianmarco Vanuzzo,[†] Domenico Stranges,[§] Xingan Wang,[∥] Jun Li,[*,‡] Hua Guo,[⊥] and Piergiorgio Casavecchia[*,†]

[†]Dipartimento di Chimica, Biologia e Biotecnologie, Università degli Studi di Perugia, 06123 Perugia, Italy

[‡]School of Chemistry and Chemical Engineering, Chongqing University, Chongqing 401331, China

[§]Dipartimento di Chimica, Sapienza - Università di Roma, 00185 Roma, Italy

[∥]Department of Chemical Physics, School of Chemistry and Materials Science, University of Science and Technology of China, Hefei, Anhui 230026, China

[⊥]Department of Chemistry and Chemical Biology, University of New Mexico, Albuquerque, New Mexico 87131, United States

Supporting Information

**ABSTRACT:** A combined experimental−theoretical study is performed to advance our understanding of the dynamics of the prototypical tetra-atom, complex-forming reaction OH + CO → H + $CO_2$, which is also of great practical relevance in combustion, Earth's atmosphere, and, potentially, Mars's atmosphere and interstellar chemistry. New crossed molecular beam experiments with mass spectrometric detection are analyzed together with the results from previous experiments and compared with quasi-classical trajectory (QCT) calculations on a new, full-dimensional potential energy surface (PES). Comparisons between experiment and theory are carried out both in the center-of-mass and laboratory frames. Good agreement is found between experiment and theory, both for product angular and translational energy distributions, leading to the conclusion that the new PES is the most accurate at present in elucidating the dynamics of this fundamental reaction. Yet, small deviations between experiment and theory remain and are presumably attributable to the QCT treatment of the scattering dynamics.

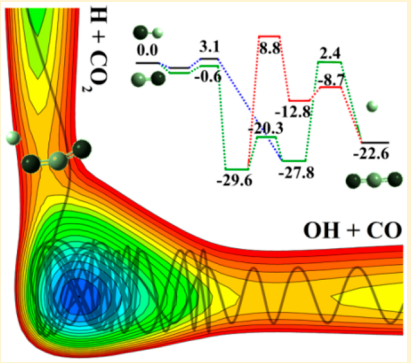


The dynamics of chemical reactions in the gas phase provides a unique proving ground for understanding chemical transformation via the breaking and forming of chemical bonds.[1] Insights from reaction dynamics studies have helped to establish key concepts in chemical reaction theory.[2−5] In recent years, the focus of chemical dynamics studies has shifted beyond the simpler atom−diatom reactions,[6,7] in pursuit of a higher level of complexity.[8−14] In this Letter, we report a combined experimental−theoretical investigation of a prototypic diatom−diatom reaction dominated by a long-lived intermediate.

The exothermic OH + CO → H + $CO_2$ reaction ($\Delta H^0_0$ = −24.0 kcal/mol, from NIST) is one of the most important reactions in hydrocarbon combustion, serving as the last and major heat-releasing step.[15] It is also a major CO removal pathway in Earth's atmosphere.[16] Furthermore, it may be important in the atmospheric chemistry of Mars[17] and of relevance in interstellar chemistry.[18] As a result, the kinetics of this reaction has been extensively studied at various temperatures and pressures.[19,20] At low temperatures, the reaction rate weakly depends on temperature, suggesting that the quantum tunneling effect does play a role in OH + CO → H + $CO_2$ reaction.[21] This reaction is also known to proceed via a reaction intermediate (*trans*- and *cis*-HOCO), as evidenced by strong pressure dependence of its rate.[22] Very recently, the HOCO intermediate has been spectroscopically identified in kinetic experiments.[23]

The dynamics of this important reaction has been investigated by several groups.[24−26] While providing the most detailed information on the dynamics, crossed molecular beam (CMB) studies have been rare. In 1993, the Perugia group reported the first measurement of the differential cross section (DCS) for the reaction OH + CO → H + $CO_2$ at the collision energy, $E_c$, of 14.1 kcal/mol using the CMB technique with mass-spectrometric (MS) detection and time-of-flight (TOF) analysis.[27] The results revealed a backward−forward $CO_2$ product angular distribution with a slight bias for forward scattering (with respect to the OH direction), confirming the formation of the HOCO intermediate with a lifetime comparable to its rotational period. The velocity distribution indicated that the internal excitation of the $CO_2$ product is minor compared with the energy released into product translational energy. The latest experiment from the same group at $E_c$ = 8.6 kcal/mol revealed similar behaviors.[28] It is

Received: December 29, 2017
Accepted: February 22, 2018
Published: February 22, 2018






DOI: 10.1021/acs.jpclett.7b03439
J. Phys. Chem. Lett. 2018, 9, 1229−1236

worth noting that in the 25 years that followed the first CMB-MS study, no other experimental techniques in the field of reaction dynamics proved to be suitable to tackle measurements of reactive DCSs for this system. This is mainly due to the relatively small reactive cross section, the low sensitivity of laser spectroscopy methods for $CO_2$ state-resolved detection, and the difficulty of generating supersonic beams of OH (OD) radicals without impurity of H(D) atoms, which have hampered so far the application of the H*-atom Rydberg tagging method as well as the H atom REMPI (resonance-enhanced multiphoton ionization) ion-imaging technique.

Theoretically, this reaction has attracted much attention due partly to the unique topography of the potential energy surface (PES);[29,30] see the Abstract graphic. The reaction path features deep HOCO potential wells flanked by an entrance channel bottleneck and near-isoenergetic exit barrier.[31] Earlier dynamical studies of this reaction[32−51] were not quantitatively correct as they suffered from poor representations of the reactive PES.[32,42] In 2012, a global PES for this reaction was developed by fitting a large number of high-level ab initio points,[52] providing a chemically accurate description of the reaction pathway and thus a much better characterization of the kinetics and reaction dynamics.[52−54] In particular, the new PES possesses a thin exit barrier, which permitted the quantum mechanical confirmation[55] of the experimentally observed deep tunneling of *cis*-HOCO to the H + $CO_2$ products.[56,57] Subsequently (in 2013), a more accurate fit of the PES was reported by Zhang and co-workers,[58] which was further improved (denoted as PES-2014 hereafter)[59] using the permutation invariant polynomial neural network (PIP-NN) method.[60] Since then, there have been several dynamical studies on this PES.[61−63] Interestingly, the calculated DCSs on the PIP-NN PES did not agree with the experimental results very well.[59] The poor agreement was speculated to originate from several possible sources, but none was confirmed.

In this Letter, we report a new CMB-MS experiment on the $^{18}$OH + CO reaction at $E_c$ = 12.6 kcal/mol, complemented with extensive quasi-classical trajectory (QCT) calculations on a new PIP-NN PES. In the new experiment, the slightly different kinematics, namely, making the OH beam slower and the CO beam faster (by seeding CO in He), has allowed us to better determine the falloff of the angular distribution at small angles (forward direction), thus removing a source of uncertainty of the previous experiments. The experimental data are analyzed together with previous data at $E_c$ = 14.5 kcal/mol to assess the reliability of the new PES presented here. (The actual average collision energy of the early experiment is not 14.1 kcal/mol, as reported originally in ref 27. On the basis of the actual beam velocities, the collision energy was recalculated to be 14.5 kcal/mol, correcting the previous numerical error, and the slightly refined best-fit reported in ref 51 has been obtained using the latter $E_c$ value. In ref 51, the experimental distributions were compared with the QCT simulations carried out at $E_c$ = 14.1 kcal/mol. The effect of changing the $E_c$ from 14.1 to 14.5 is however rather small. In the present work, the QCT calculations have been performed at exactly the experimental collision energy of 14.5 kcal/mol.) Good, although not perfect, agreement between experiment and theory is reached, thus advancing our understanding of this important reaction.

The experiments were carried out using a "universal" CMB apparatus, which has been described elsewhere.[64,65] Details of the experiments are given in the Supporting Information (SI). By crossing at 90° a seeded beam of $^{18}$OH (peak velocity of 2787 m/s), having a known rotational distribution, with a seeded beam of CO (peak velocity of 1356 m/s), the resulting collision energy is $E_c$ = 12.6 kcal/mol. As in previous experiments, the use of isotopically labeled $^{18}$OH permitted us to detect $CO_2$ at $m/z$ = 46, for which the inherent detector background is much lower than that at $m/z$ = 44. With respect to the kinematics of the previous experiment at $E_c$ = 14.5 kcal/mol (where the CM angle, $\Theta_{CM}$, was about 27°),[51] in the present work, because of the somewhat lower OH velocity and larger CO velocity, the CM angle has moved to $\Theta_{CM}$ = 36°, and this has permitted us to measure the $CO_2$ product angular distribution, $N(\Theta)$, more accurately by observing clearly its complete falloff to zero at both smaller and larger angles than the CM angle.

Theoretically, we develop a new PES (denoted as PES-2018 hereafter) with the same data set as that used in PES-2014.[59] Different from the segmented NN fits in PES-2014, PES-2018 is fit using one NN for all regions with PIPs up to second order, resulting in 17 input variables. The two NN hidden layers are chosen to have 50 and 80 neurons, resulting in 5061 parameters. Its root-mean-square errors for the train/validation/test/total sets and maximum deviation are 5.2/6.4/8.9/5.5 and 209.5 meV, respectively. Because the gradient of the PES is obtained analytically, PES-2018 is about 5−10 times faster than PES-2014. Using PES-2018, the cross sections were computed using the QCT method implemented in VENUS[66] as quantum DCS calculations are still beyond our capabilities for this complex-forming reaction. Between $3 \times 10^6$ and $1 \times 10^7$ trajectories were calculated at collisional energies of 7.0, 11.5, 13.0, 13.9, 14.5, 17.0, and 22.0 kcal/mol. Simulations of the data at $E_c$ = 12.6 kcal/mol have been done using the QCT results obtained at $E_c$ = 13.0 kcal/mol, which is considered a very good approximation. Additional details are given in the SI.

Figure 1 depicts with solid dots the measured laboratory (LAB) angular distribution of the $CO_2$ ($m/z$ = 46) product at $E_c$ = 12.6 kcal/mol (top two panels) and those obtained previously[27,51] at $E_c$ = 14.5 kcal/mol (bottom two panels), together with the best-fit curves and the QCT simulations (see below). Error bars represent a ±1 standard deviation. The QCT simulation at $E_c$ = 14.5 kcal/mol was performed by taking into account the contribution of the various populated OH rotational levels, $N_{OH}$, as described previously[51] (see the SI for details). Because OH rotational excitation had little effect, the QCT calculations at the lower $E_c$ were only done for $N_{OH}$ = 1. Similarly, CO rotational excitation has little impact on the results. As can be seen from Figure 1, the unfavorable kinematics, resulting from detection of the (heavy) $CO_2$ moiety, confines the $CO_2$ reactive scattering to a relatively narrow range of LAB angles, thus limiting the resolution of the experiments.

Figure 2 shows the TOF spectrum recorded at a CM angle of 36° at $E_c$ = 12.6 kcal/mol (top panel) and the corresponding TOF spectra at selected angles at $E_c$ = 14.5 kcal/mol (bottom panel), with the best-fit (dashed line) and the QCT simulation (solid line) (in the theoretical simulation at the higher $E_c$, the contributions from the various $^{18}$OH rotational levels are also included as for the product angular distribution of Figure 1).

The solid lines superimposed on the experimental points in the first and third panels of Figure 1 and the dashed lines superimposed on the TOF spectra of Figure 2 are the curves calculated when using the best-fit CM functions of Figure 3. As usual, quantitative information is extracted from the raw LAB data by moving from the LAB coordinate system to the CM



DOI: 10.1021/acs.jpclett.7b03439
J. Phys. Chem. Lett. 2018, 9, 1229−1236

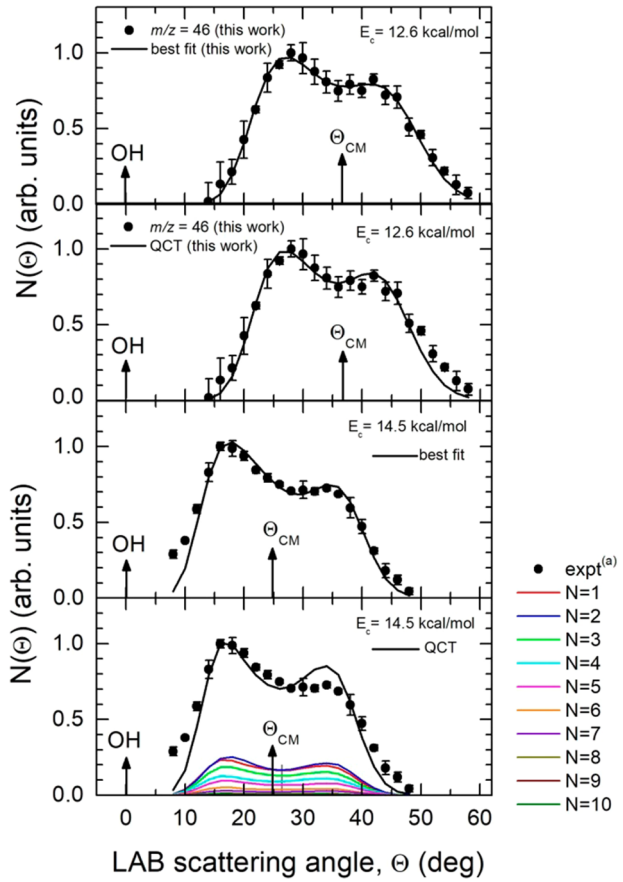


**Figure 1.** Solid dots: $CO_2$ ($m/z$ = 46) product angular distribution from the $^{18}OH$ + CO reaction at $E_c$ = 12.6 kcal/mol (top two panels) and $E_c$ = 14.5 kcal/mol (bottom two panels) [(a) expt. from refs 27 and 51]. Solid lines: Best-fit curves (first and third panels from top); simulation using the product CM angular and translational energy distributions obtained from the present QCT calculations on PES-2018 (second and fourth panels). For $E_c$ = 14.5 kcal/mol in the QCT simulations, the relative contributions from the main populated rotational states of the $^{18}OH$ reactant are also indicated (see text).

one and analyzing the product angular, $T(\theta)$, and translational energy, $P(E'_T)$, distributions into which the CM product flux, $I_{CM}(\theta,E'_T) = T(\theta)P(E'_T)$, can be factorized.[27,28] The best-fit CM functions are actually derived by a forward convolution fit of the product LAB angular, $N(\Theta)$, and TOF, $N(\Theta,t)$, distributions at $m/z$ = 46 according to the relation $N_{LAB}(\theta,v) = I_{CM}(\theta,u)v/u^2$, where $v$ and $u$ are product LAB and CM velocities, respectively, and averaging over the experimental conditions (beam velocity and angular spreads and detector acceptance angle). During the experimental averaging of the CM functions, also the energy dependence of the integral cross section (ICS) was taken into account, as obtained from the present QCT calculations on the new PES (see Figure 4 for the reaction of OH($N_{OH}$ = 1) and Figure S4 for the various OH rotational levels). The assumption that the $T(\theta)$ and $P(E'_T)$ functions are uncoupled (there was no need to couple them in the fitting of the data) was verified in similar QCT calculations using other PESs, as described in refs 51, 66, and is corroborated by the present QCT calculations, which found as well negligible angular dependence of the $P(E'_T)$ distribution.

The best-fit $CO_2$ $T(\theta)$ and product $P(E'_T)$ distributions are shown on the left-hand side and right-hand side, respectively of the top ($E_c$ = 12.6 kcal/mol) and bottom ($E_c$ = 14.5 kcal/mol) panels of Figure 3 as red continuous lines, with the error bounds of their determination indicated with shaded areas. In the same graphs, the theoretical QCT results are also shown for four selected rotational levels of OH (see below).

As can be seen from Figure 3, the best-fit CM angular distribution at $E_c$ = 12.6 kcal/mol is distributed all over the 0–180° CM angular range but with more intensity in the forward direction (with respect to the incoming OH reactant direction, $\theta$ = 0°) than in the backward one. The $T(\theta = 180°)/T(\theta = 0°)$ intensity ratio is 0.76/1.00, which is in line with the previous determination[51] at the higher $E_c$ of 14.5 kcal/mol, for which $T(\theta = 180°)/T(\theta = 0°)$ = 0.63/1.00. The higher $T(\theta)$ anisotropy at the higher $E_c$ can be interpreted in terms of the "osculating model" of chemical reactions,[67] which allows us to make an approximate estimate of the average lifetime, $\tau$, of the HOCO complex intermediate (see the SI). A lower limit to the complex lifetime is calculated to be 0.5 and 0.8 ps for the higher and lower $E_c$ experiments, respectively. The corresponding values obtained directly from the present QCT calculations are 0.98 and 1.45 ps, respectively.

The average fraction of energy released as product translational energy, $f_T$, was experimentally found to be quite high (0.60 and 0.64 for the lower and higher $E_c$ experiments, respectively). The experimental average product translational energy, $\langle E_T \rangle$, is 22.3 kcal/mol at $E_c$ = 12.6 and 25.0 kcal/mol at $E_c$ = 14.5 kcal/mol. These values are very close to the value of the barrier height (with respect to the product asymptote) of about 25 kcal/mol in the exit channel of the reaction. The post-transition-state PES is quite repulsive, consistent with the dominant energy release into the product recoil.

The QCT $T(\theta)$, reported in the top panel of Figure 3 as a black line ($E_c$ = 12.6 kcal/mol), also shows a forward–backward anisotropy, similar to the experimental one; however, the overall shape differs somewhat from the experimental curve, exhibiting a slightly higher intensity in the sideways direction, although almost within the error bounds of the experimental determination. In particular, at the higher $E_c$ (lower four panels), the anisotropy from QCT for the indicated $N_{OH}$ is at the upper limit of the experimental error bounds. The lower QCT anisotropy and the more pronounced sideways scattering with respect to the best-fit $T(\theta)$ are responsible for the resulting deviation of the simulated curve in the LAB frame with respect to experiment and the best-fit curve (see Figure 1).

As far as the product translational energy distribution is concerned, we notice in Figure 3 that the QCT $P(E'_T)$ is somewhat colder than the experimental one, especially at the higher $E_c$ for all $N_{OH}$. Specifically, at the lower and higher $E_c$, the average product translational energy from the QCT calculations is 21.36 and 22.05 kcal/mol, which are about 5 and 12%, respectively, lower than the experimental determinations. These deviations, at least in part, are responsible of the slightly narrower QCT $N(\Theta)$ distribution with respect to experiment, noticeable at both the lower $E_c$ (see Figure 1, second panel from top) and higher $E_c$ (see Figure 1, bottom panel).

Part of the reason for the deviation between experiment and theory could be due to the effect of the rotational energy (see Figure S6). However, although $N_{OH}$ = 10 could contribute for more than 2 kcal/mol to the total available energy, its population is estimated to be a few percent in the OH reactant beam, with most of the population residing in the lowest few rotational levels (see Table S1 in the SI). The effect of OH



DOI: 10.1021/acs.jpclett.7b03439
J. Phys. Chem. Lett. 2018, 9, 1229–1236

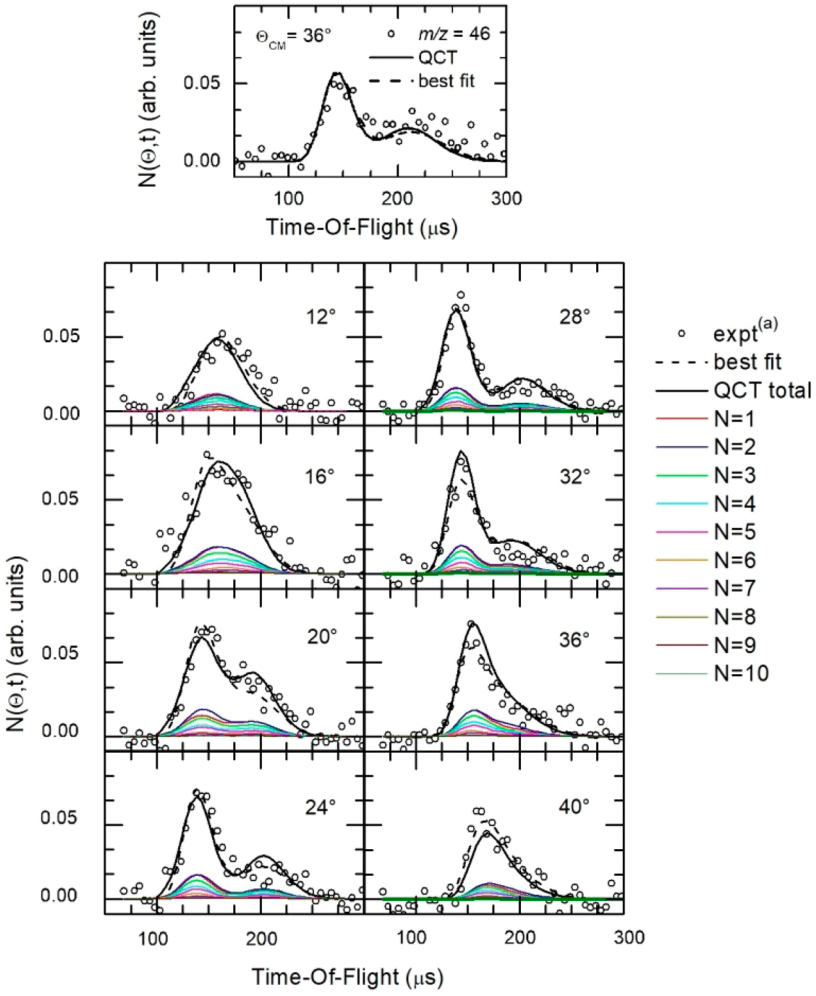


**Figure 2.** Open circles: Product TOF distribution of the $CO_2$ product at a CM angle of 36° for $E_c$ = 12.6 kcal/mol and at selected LAB angles for $E_c$ = 14.5 kcal/mol. [(a) expt. from refs 27 and 51]. Dashed line: Best-fit. Solid line: Simulation using the present QCT results on PES-2018 (see text).

rotational excitation using the new PES was explored only at the higher $E_c$ = 14.5 kcal/mol. Interestingly, it turned out to be modest, as already inferred from previous simulations at this $E_c$ using other PESs for the OH + CO reaction[51] (see the SI for details).

As previously noted,[51] because of the uncertainties associated with the derivation of the experimental best-fit CM functions from the measured raw data, a more straightforward comparison can be performed by transforming the theoretical CM functions into the LAB distributions, so that a direct comparison with the raw LAB data can be obtained and uncertainties associated with the derivation of the best-fit functions avoided. Such a transformation has to be carried out by taking into account the experimental conditions (crossing angle, beam velocities) and averaging over the experimental parameters (beam velocity distributions, angular divergences, detector aperture). The QCT simulated LAB angular distributions (with the different, weighted OH rotational contributions indicated) versus the experimental data are shown in the bottom panel of Figure 1 (at $E_c$ = 14.5 kcal/mol). The corresponding TOF spectra simulated by the QCT calculations are shown in Figure 2. The state of comparison between experiment and QCT predictions is nearly indistinguishable (for the experiment at $E_c$ = 14.5 kcal/mol) between the case in which the separate, weighted contributions of all $N_{OH}$ levels are considered and the case where only $N_{OH}$ = 1 was considered. There is only a little improvement (not shown) on the reproduction of the wings of the angular distribution, which is due to the fact that the $P(E'_T)$s of high $N_{OH}$ levels have a tail and a peak slightly displaced toward a higher value of $E_c$. We remind that LAB angular and TOF distributions are mostly affected by the rise of the $P(E'_T)$s and their peak positions, with little sensitivity to the tails. In fact, at the $E_c$ of 14.5 kcal/mol, the discrepancy between the QCT angular distribution and experiment (see Figure 1, bottom panel) (different forward and backward peak heights) essentially did not vary by considering also the high $N_{OH}$ contributions, especially because the ICS weight decreases with the increase of $N_{OH}$ (see Table S1 in the SI). Noticeably, also the TOF distributions (at the higher $E_c$) show some difference between experiment and theory, but because of the finite signal-to-noise, it is difficult to draw any quantitative conclusion (although the QCT TOF curves appear to perform slightly better than the best-fit ones at some angles).

A more likely reason for the deviation between the experimental and QCT $P(E'_T)$ distributions, and perhaps also $T(\theta)$ distributions (see, for instance, ref 68) (Figure 3), could presumably be ascribed to the neglect of quantum effects, such as tunneling, zero-point energy, and resonances in the QCT approach. Tunneling is known to play an important role in this



DOI: 10.1021/acs.jpclett.7b03439
J. Phys. Chem. Lett. 2018, 9, 1229−1236

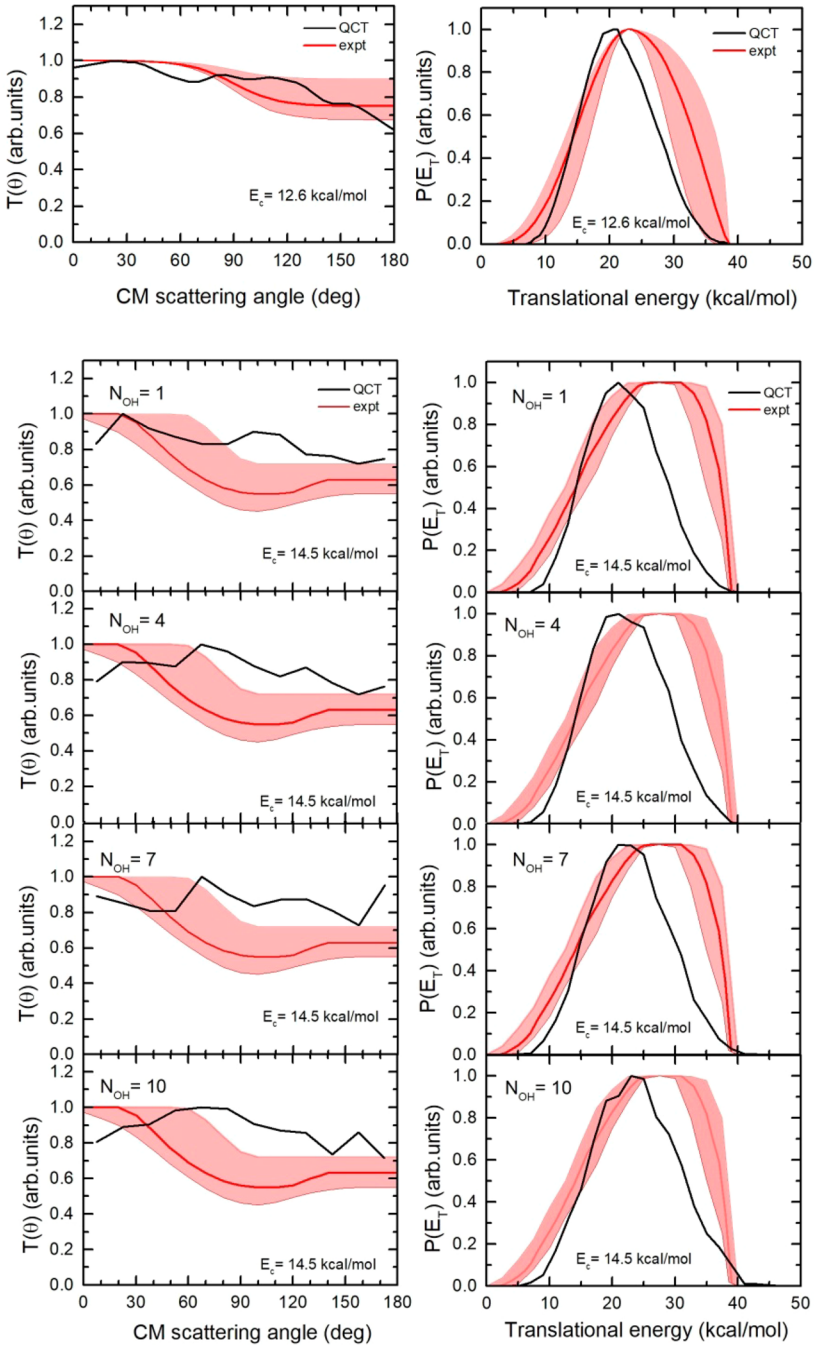


**Figure 3.** Best-fit CM $CO_2$ angular distributions (lhs panels) and product translational energy distributions (rhs panels) for the $^{18}OH$ + CO reaction at $E_c$ = 12.6 kcal/mol (top panel) and $E_c$ = 14.5 kcal/mol (bottom panels). Red: Best-fit functions, with shaded areas delimiting the error bound of the determination. Black lines: $T(\theta)$ and $P(E'_T)$ distributions from the QCT calculations for only $N_{OH}$ = 1 at $E_c$ = 12.6 kcal/mol and for four exemplary values (indicated) of $N_{OH}$ at $E_c$ = 14.5 kcal/mol (see text).

reaction, as evidenced by near-constant rate coefficients at low temperatures.[21] Quantum mechanical treatments of the tunneling dynamics have revealed the significance of this quantum effect in kinetics and dynamics.[55,62,69,70] In addition, zero-point leakage is a well-known problem in QCT. Finally, resonances in this reaction are also quite pronounced, as demonstrated by recent quantum scattering calculations.[54,63]

In summary, a new joint experimental−theoretical study for the title reaction is reported. The newly measured DCS shows scattering in both the forward and backward directions, with a slight forward bias, confirming the anisotropy observed in previous CMB experiments. The product angular and velocity distributions measured here and in a previous work are satisfactorily reproduced by QCT on a new globally accurate PES. The improved agreement between theory and experiment indicates a more in-depth understanding of the dynamics of this prototypical reaction. The remaining differences are attributed to the lack of quantum effects in the QCT treatment. Further improvements in the elucidation of the OH + CO reaction dynamics can be expected from quantum scattering calculations of the dynamics as well as from higher-resolution and/or state-resolved CMB experiments, when these become available.



DOI: 10.1021/acs.jpclett.7b03439
J. Phys. Chem. Lett. 2018, 9, 1229−1236

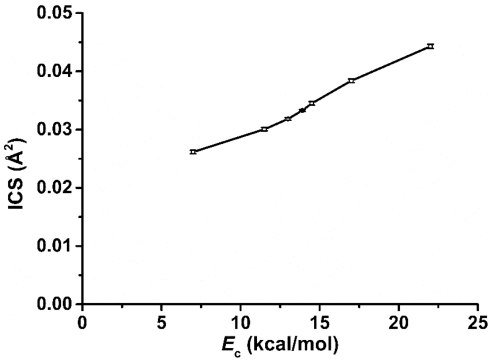


**Figure 4.** Dots: ICSs for the reaction $^{18}OH + CO$ as a function of collision energy (the solid line has been drawn to guide the eye and error bars shown).

## ■ ASSOCIATED CONTENT

### Supporting Information

The Supporting Information is available free of charge on the ACS Publications website at DOI: 10.1021/acs.jpclett.7b03439.

Details of the PES fitting and QCT calculations; additional results; Figures S1−S10 and Table S1, showing the fwhm spread of the relative translational energies of the reactants, opacity function, residence time distribution, integral reactive cross sections, product angular distributions, translational energy distributions, relative integral and differential cross sections, effect of rotational excitation on the translations energy distributions, and effect of OH rotational excitation on ICS (PDF)

## ■ AUTHOR INFORMATION


### Corresponding Authors

*E-mail: jli15@cqu.edu.cn (J.L.).

*E-mail: piergiorgio.casavecchia@unipg.it (P.C.).

### ORCID

Xingan Wang: 0000-0002-1206-7021

Jun Li: 0000-0003-2392-8322

Hua Guo: 0000-0001-9901-053X

Piergiorgio Casavecchia: 0000-0003-1934-7891


### Author Contributions

#A.C. and D.L. contributed equally.

### Notes

The authors declare no competing financial interest.

## ■ ACKNOWLEDGMENTS

A.C., N.B., G.V., and P.C. acknowledge financial support from the "Fondazione Cassa Risparmio Perugia Italy" (Project code: 2015.0331.021 Scientific and Technological Research) and the University of Perugia ("Fondo Ricerca di Base 2014"). Partial support from COST Action CM1404 (Chemistry of Smart Energy Carriers and Technologies − SMARTCATS) is also acknowledged. D.L. and J.L. are supported by the National Natural Science Foundation of China (Contract No. 21573027 to J.L.). H.G. thanks the U.S. Department of Energy (DE-SC0015997) for partial support. X.W. acknowledges the University of Perugia for a Visiting Scholarship grant in July 2016 (within the entrance Mobility Program of Researchers of International Fame). Support from Italian MIUR and Università degli Studi di Perugia is acknowledged within the program "Dipartimento di Eccellenza − 2018-2022" - project AMIS.

## ■ REFERENCES


(1) Levine, R. D. *Molecular Reaction Dynamics*; Cambridge University Press: Cambridge, U.K., 2005.

(2) Polanyi, J. C. Concepts in Reaction Dynamics. *Acc. Chem. Res.* **1972**, *5*, 161−168.

(3) Crim, F. F. Vibrational State Control of Bimolecular Reactions: Discovering and Directing the Chemistry. *Acc. Chem. Res.* **1999**, *32*, 877−884.

(4) Liu, K. Crossed-Beam Studies of Neutral Reactions: State-Specific Differential Cross Sections. *Annu. Rev. Phys. Chem.* **2001**, *52*, 139−164.

(5) Guo, H.; Jiang, B. The Sudden Vector Projection Model for Reactivity: Mode Specificity and Bond Selectivity Made Simple. *Acc. Chem. Res.* **2014**, *47*, 3679−3685.

(6) Casavecchia, P.; Balucani, N.; Alagia, M.; Cartechini, L.; Volpi, G. G. Reactive Scattering of Oxygen and Nitrogen Atoms. *Acc. Chem. Res.* **1999**, *32*, 503−511.

(7) Yang, X. State-to-State Dynamics of Elementary Bimolecular Reactions. *Annu. Rev. Phys. Chem.* **2007**, *58*, 433−459.

(8) Balucani, N.; Capozza, G.; Leonori, F.; Segoloni, E.; Casavecchia, P. Crossed Molecular Beam Reactive Scattering: from Simple Triatomic to Multichannel Polyatomic Reactions. *Int. Rev. Phys. Chem.* **2006**, *25*, 109−163.

(9) Nyman, G.; Yu, H.-G. Quantum Approaches to Polyatomic Reaction Dynamics. *Int. Rev. Phys. Chem.* **2013**, *32*, 39−95.

(10) Czakó, G.; Bowman, J. M. Reaction Dynamics of Methane with F, O, Cl, and Br on Ab Initio Potential Energy Surfaces. *J. Phys. Chem. A* **2014**, *118*, 2839−2864.

(11) Li, J.; Jiang, B.; Song, H.; Ma, J.; Zhao, B.; Dawes, R.; Guo, H. From Ab Initio Potential Energy Surfaces to State-Resolved Reactivities: The X + $H_2O$ ↔ HX + OH (X = F, Cl, and $O(^3P)$) Reactions. *J. Phys. Chem. A* **2015**, *119*, 4667−4687.

(12) Zhang, D. H.; Guo, H. Recent Advances in Quantum Dynamics of Bimolecular Reactions. *Annu. Rev. Phys. Chem.* **2016**, *67*, 135−158.

(13) Liu, K. Vibrational Control of Bimolecular Reactions with Methane with Mode-, Bond-, and Stereo-Selectivity. *Annu. Rev. Phys. Chem.* **2016**, *67*, 91−111.

(14) Pan, H.; Liu, K.; Caracciolo, A.; Casavecchia, P. Crossed Beam Polyatomic Reaction Dynamics: Recent Advances and New Insights. *Chem. Soc. Rev.* **2017**, *46*, 7517−7547.

(15) Miller, J. A.; Kee, R. J.; Westbrook, C. K. Chemical-Kinetics and Combustion Modeling. *Annu. Rev. Phys. Chem.* **1990**, *41*, 345−387.

(16) Röckmann, T.; Brenninkmeijer, C. A. M.; Saueressig, G.; Bergamaschi, P.; Crowley, J. N.; Fischer, H.; Crutzen, P. J. Mass-Independent Oxygen Isotope Fractionation in Atmospheric CO as a Result of the Reaction CO + OH. *Science* **1998**, *281*, 544−546.

(17) Liu, Y.; Sander, S. P. Rate Constant for the OH + CO Reaction at Low Temperatures. *J. Phys. Chem. A* **2015**, *119*, 10060−10066.

(18) Goumans, T. P. M.; Uppal, M. A.; Brown, W. A. Formation of $CO_2$ on a Carbonaceous Surface: a Quantum Chemical Study. *Mon. Not. R. Astron. Soc.* **2008**, *384*, 1158−1164.

(19) Fulle, D.; Hamann, H. F.; Hippler, H.; Troe, J. High Pressure Range of Addition Reactions of HO. II. Temperature and Pressure Dependence of the Reaction HO+CO ⇔ HOCO ⇔ H+$CO_2$. *J. Chem. Phys.* **1996**, *105*, 983−1000.

(20) Golden, D. M.; Smith, G. P.; McEwen, A. B.; Yu, C.-L.; Eiteneer, B.; Frenklach, M.; Vaghjiani, G. L.; Ravishankara, A. R.; Tully, F. P. OH(OD) + CO: Measurements and an Optimized RRKM Fit. *J. Phys. Chem. A* **1998**, *102*, 8598−8606.

(21) Frost, M. J.; Sharkey, P.; Smith, I. W. M. Reaction Between Hydroxyl (Deuteroxyl) Radicals and Carbon Monoxide at Temperatures Down to 80 K: Experiment and Theory. *J. Phys. Chem.* **1993**, *97*, 12254−12259.

(22) Smith, I. W. M.; Zellner, R. Rate Measurements of Reactions of OH by Resonance Absorption, Part 2. Reaction of OH with CO, $C_2H_4$, and $C_2H_2$. *J. Chem. Soc., Faraday Trans. 2* **1973**, *69*, 1617−1627.




DOI: 10.1021/acs.jpclett.7b03439
*J. Phys. Chem. Lett.* 2018, 9, 1229−1236

(23) Bjork, B. J.; Bui, T. Q.; Heckl, O. H.; Changala, P. B.; Spaun, B.; Heu, P.; Follman, D.; Deutsch, C.; Cole, G. D.; Aspelmeyer, M.; et al. Direct Frequency Comb Measurement of OD + CO → DOCO Kinetics. *Science* **2016**, *354*, 444−448.
(24) Dreier, T.; Wolfrum, J. Direct Study of the Reaction of Vibrationally Excited CO Molecules with OH Radicals. *Symp. Combust., [Proc.]* **1981**, *18*, 801−809.
(25) Frost, M. J.; Salh, J. S.; Smith, I. W. M. Vibrational-State Distribution of $CO_2$ Produced in the Reaction Between OH Radicals and CO. *J. Chem. Soc., Faraday Trans.* **1991**, *87*, 1037−1038.
(26) Koppe, S.; Laurent, T.; Volpp, H. R.; Wolfrum, J.; Naik, P. D. Absolute Reactive Cross Sections for the Reaction OH + CO → H + $CO_2$. *Symp. Combust., [Proc.]* **1996**, *26*, 489−495.
(27) Alagia, M.; Balucani, N.; Casavecchia, P.; Stranges, D.; Volpi, G. G. Crossed Beam Studies of Four-Atom Reactions: the Dynamics of OH+CO. *J. Chem. Phys.* **1993**, *98*, 8341−8344.
(28) Casavecchia, P.; Balucani, N.; Volpi, G. G. Reactive Scattering of O($^3$P, $^1$D), Cl($^2$P) and OH Radicals. In *Chemical Dynamics and Kinetics of Small Free Radicals*; Wagner, A. F., Liu, K., Eds.; World Scientific: Singapore, 1995; Vol. *Part I*, pp 365−437.
(29) Francisco, J. S.; Muckerman, J. T.; Yu, H.-G. HOCO Radical Chemistry. *Acc. Chem. Res.* **2010**, *43*, 1519−1526.
(30) Guo, H. Quantum Dynamics of Complex-Forming Bimolecular Reactions. *Int. Rev. Phys. Chem.* **2012**, *31*, 1−68.
(31) Schatz, G. C.; Fitzcharles, M. S.; Harding, L. B. State-to-State Chemistry with Fast Hydrogen Atoms. *Faraday Discuss. Chem. Soc.* **1987**, *84*, 359−369.
(32) Kudla, K.; Schatz, G. C.; Wagner, A. F. A Quasiclassical Trajectory Study of the OH+CO Reaction. *J. Chem. Phys.* **1991**, *95*, 1635−1647.
(33) Kudla, K.; Koures, A.; Harding, L. B.; Schatz, G. C. A Quasiclassical Trajectory Study of OH Rotational Excitation in OH +CO Collisions Using Ab Initio Potential Surfaces. *J. Chem. Phys.* **1992**, *96*, 7465−7473.
(34) Schatz, G. C.; Dyck, J. A Reduced Dimension Quantum Reactive Scattering Study of OH + CO → H + $CO_2$. *Chem. Phys. Lett.* **1992**, *188*, 11−15.
(35) Clary, D. C.; Schatz, G. C. Quantum and Quasiclassical Calculations on the OH + CO → $CO_2$ + H Reaction. *J. Chem. Phys.* **1993**, *99*, 4578−4589.
(36) Zhang, D. H.; Zhang, J. Z. H. Quantum Calculations of Reaction Probabilities for HO + CO → H + $CO_2$ and Bound States of HOCO. *J. Chem. Phys.* **1995**, *103*, 6512−6519.
(37) Goldfield, E. M.; Gray, S. K.; Schatz, G. C. Quantum Dynamics of a Planar Model for the Complex Forming OH + CO → H + $CO_2$ Reaction. *J. Chem. Phys.* **1995**, *102*, 8807−8817.
(38) Kudla, K.; Schatz, G. C. Product State Distributions in Chemical Reactions: The Reaction OH + CO → H + $CO_2$. In *The Chemical Dynamics and Kinetics of Small Radicals*; Liu, K., Wagner, A. F., Eds. World Scientific: Singapore, 1995; p 438.
(39) Dzegilenko, F.; Bowman, J. M. Recovering a Full Dimensional Quantum Rate Constant from a Reduced Dimensionality Calculation: Application to the OH+CO → H+$CO_2$ Reaction. *J. Chem. Phys.* **1996**, *105*, 2280−2286.
(40) McCormack, D. A.; Kroes, G.-J. Full-Dimensional Quantal Initial State-Selected Reaction Probabilities (J = 0) for the Reaction OH(v = 0,j = 0) + CO(v = 0,j = 0) → $CO_2$ + H. *Chem. Phys. Lett.* **2002**, *352*, 281−287.
(41) McCormack, D. A.; Kroes, G.-J. Converged Five-Dimensional Quantun Calculations for OH + CO → H + $CO_2$. *J. Chem. Phys.* **2002**, *116*, 4184−4191.
(42) Lakin, M. J.; Troya, D.; Schatz, G. C.; Harding, L. B. A Quasiclassical Trajectory Study of the Reaction OH + CO → H + $CO_2$. *J. Chem. Phys.* **2003**, *119*, 5848−5859.
(43) Valero, R.; McCormack, D. A.; Kroes, G.-J. New Results for the OH(v = 0,j = 0) + CO(v = 0,j = 0) → H + $CO_2$ Reaction: Five and Full-Dimensional Quantum Dynamical Study on Several Potential Energy Surfaces. *J. Chem. Phys.* **2004**, *120*, 4263−4272.
(44) Medvedev, D. M.; Gray, S. K.; Goldfield, E. M.; Lakin, M. J.; Troya, D.; Schatz, G. C. Quantum Wave Packet and Quasiclassical Trajectory Studies of OH + CO: Influence of the Reactant Channel Well on Thermal Rate Constants. *J. Chem. Phys.* **2004**, *120*, 1231−1238.
(45) Valero, R.; Kroes, G.-J. Role of CO Vibration in the Complex-Forming OH + CO → H + $CO_2$ Reaction. *Phys. Rev. A: At., Mol., Opt. Phys.* **2004**, *70*, 040701.
(46) Valero, R.; Kroes, G.-J. Theoretical Reaction Dynamics Study of the Effect of Vibrational Excitation of CO on the OH + CO → H + $CO_2$ Reaction. *J. Phys. Chem. A* **2004**, *108*, 8672−8681.
(47) Garcia, E.; Saracibar, A.; Zuazo, L.; Laganà, A. A Detailed Trajectory Study of the OH + CO → H + $CO_2$ Reaction. *Chem. Phys.* **2007**, *332*, 162−175.
(48) Liu, S.; Xu, X.; Zhang, D. H. Communication: State-to-State Quantum Dynamics Study of the OH + CO → H + $CO_2$ Reaction in Full Dimensions (J = 0). *J. Chem. Phys.* **2011**, *135*, 141108.
(49) Liu, S.; Xu, X.; Zhang, D. H. A Full-Dimensional Time-Dependent Wave Packet Study of the OH+CO → H+$CO_2$ Reaction. *Theor. Chem. Acc.* **2012**, *131*, 1068.
(50) Wang, C.; Liu, S.; Zhang, D. H. Effects of Reagent Vibrational Excitation on the State-to-State Quantum Dynamics of the OH + CO → H + $CO_2$ Reaction in Six Dimensions (J = 0). *Chem. Phys. Lett.* **2012**, *537*, 16−20.
(51) Laganà, A.; Garcia, E.; Paladini, A.; Casavecchia, P.; Balucani, N. The Last Mile of Molecular Reaction Dynamics Virtual Experiments: The Case of the OH(N = 1−10) + CO(j = 0−3) Reaction. *Faraday Discuss.* **2012**, *157*, 415−436.
(52) Li, J.; Wang, Y.; Jiang, B.; Ma, J.; Dawes, R.; Xie, D.; Bowman, J. M.; Guo, H. Communication: A Chemically Accurate Global Potential Energy Surface for the HO + CO → H + $CO_2$ Reaction. *J. Chem. Phys.* **2012**, *136*, 041103.
(53) Li, J.; Xie, C.; Ma, J.; Wang, Y.; Dawes, R.; Xie, D.; Bowman, J. M.; Guo, H. Quasi-Classical Dynamics of the HO + CO → H + $CO_2$ Reaction on a New Ab Initio Based Potential Energy Surface. *J. Phys. Chem. A* **2012**, *116*, 5057−5067.
(54) Ma, J.; Li, J.; Guo, H. Quantum Dynamics of the HO + CO → H + $CO_2$ Reaction on an Accurate Potential Energy Surface. *J. Phys. Chem. Lett.* **2012**, *3*, 2482−2486.
(55) Ma, J.; Li, J.; Guo, H. Tunneling Facilitated Dissociation to H + $CO_2$ in $HOCO^-$ Photodetachment. *Phys. Rev. Lett.* **2012**, *109*, 063202.
(56) Johnson, C. J.; Continetti, R. E. Dissociative Photodetachment Studies of the Cooled $HOCO^-$ Anions Revealing Dissociation Below the Barrier to H + $CO_2$. *J. Phys. Chem. Lett.* **2010**, *1*, 1895−1899.
(57) Johnson, C. J.; Poad, B. L. J.; Shen, B. B.; Continetti, R. E. Communication: New Insight Into the Barrier Governing $CO_2$ Formation from OH + CO. *J. Chem. Phys.* **2011**, *134*, 171106.
(58) Chen, J.; Xu, X.; Xu, X.; Zhang, D. H. Communication: An Accurate Global Potential Energy Surface for the OH + CO → H + $CO_2$ Reaction Using Neural Networks. *J. Chem. Phys.* **2013**, *138*, 221104.
(59) Li, J.; Chen, J.; Zhang, D. H.; Guo, H. Quantum and Quasi-Classical Dynamics of the OH + CO → H + $CO_2$ Reaction on a New Permutationally Invariant Neural Network Potential Energy Surface. *J. Chem. Phys.* **2014**, *140*, 044327.
(60) Jiang, B.; Li, J.; Guo, H. Potential Energy Surfaces from High Fidelity Fitting of Ab Initio Points: The Permutation Invariant Polynomial-Neural Network Approach. *Int. Rev. Phys. Chem.* **2016**, *35*, 479−506.
(61) Wagner, A. F.; Dawes, R.; Continetti, R. E.; Guo, H. Theoretical/Experimental Comparison of Deep Tunneling Decay of Quasi-Bound H(D)OCO to H(D) + $CO_2$. *J. Chem. Phys.* **2014**, *141*, 054304.
(62) Wang, J.; Li, J.; Ma, J.; Guo, H. Full-Dimensional Characterization of Photoelectron Spectra of $HOCO^-$ and $DOCO^-$ and Tunneling Facilitated Decay of HOCO Prepared by Anion Photodetachment. *J. Chem. Phys.* **2014**, *140*, 184314.
(63) Liu, S.; Chen, J.; Fu, B.; Zhang, D. H. State-to-State Quantum Versus Classical Dynamics Study of the OH + CO → H + $CO_2$


DOI: 10.1021/acs.jpclett.7b03439
*J. Phys. Chem. Lett.* 2018, 9, 1229−1236

Reaction in Full Dimensions (J = 0): Checking the Validity of the Quasi-Classical Trajectory Method. *Theor. Chem. Acc.* **2014**, *133*, 1558.
(64) Casavecchia, P.; Leonori, F.; Balucani, N.; Petrucci, R.; Capozza, G.; Segoloni, E. Probing the Dynamics of Polyatomic Multichannel Elementary Reactions by Crossed Molecular Beam Experiments with Soft Electron-Ionization Mass Spectrometric Detection. *Phys. Chem. Chem. Phys.* **2009**, *11*, 46−65.
(65) Casavecchia, P.; Leonori, F.; Balucani, N. Reaction Dynamics of Oxygen Atoms with Unsaturated Hydrocarbons from Crossed Molecular Beam Studies: Primary Products, Branching Ratios and Role of Intersystem Crossing. *Int. Rev. Phys. Chem.* **2015**, *34*, 161−204.
(66) Laganá, A.; Balucani, N.; Crocchianti, S.; Casavecchia, P.; Garcia, E.; Saracibar, A. An Extension of the Molecular Simulator GEMS to Calculate the Signal of Crossed Beam Experiments. *Computational Science and Its Applications - ICCSA 2011: Part III*; Springer: Berlin, 2011; pp 453−465.
(67) Herschbach, D. Molecular Dynamics of Elementary Chemical Reactions. In *Nobel Lectures in Chemistry 1981−1990*; Malmstrom, B. G., Ed. World Scientic Publishing: Singapore, 1993; pp 265−314.
(68) Balucani, N.; Cartechini, L.; Capozza, G.; Segoloni, E.; Casavecchia, P.; Volpi, G. G.; Aoiz, F. J.; Banares, L.; Honvault, P.; Launay, J.-M. Quantum Effects in the Differential Cross Section for the Insertion Reaction $N(^2D) + H_2$. *Phys. Rev. Lett.* **2002**, *89*, 013201.
(69) Chen, W.-C.; Marcus, R. A. On the Theory of the CO + OH Reaction, Included H and C Kinetic Isotope Effects. *J. Chem. Phys.* **2005**, *123*, 094307.
(70) Nguyen, T. L.; Xue, B. C.; Weston, R. E., Jr.; Barker, J. R.; Stanton, J. F. Reaction of HO with CO: Tunneling is Indeed Important. *J. Phys. Chem. Lett.* **2012**, *3*, 1549−1553.



DOI: 10.1021/acs.jpclett.7b03439
*J. Phys. Chem. Lett.* 2018, 9, 1229−1236